ARPHA Preprints

PENSOFT

PREPRINT

Author-formatted, not peer-reviewed document posted on 13/05/2022

DOI: https://doi.org/10.3897/arphapreprints.e86382

Molecular and morphological description of four new *Ethmostigmus* Pocock, 1898 (Chilopoda, Scolopendromorpha, Scolopendridae) species from China, with a key to Chinese species

Chao Jiang, Juan Liu, Yangyang Pan, Tianyun Chen, Luqi Huang

Molecular and morphological descriptions of four new species of *Ethmostigmus* Pocock, 1898 (Chilopoda, Scolopendromorpha, Scolopendridae) from China, with a key to the Chinese species

Chao Jiang[1*], Juan Liu[1], Yangyang Pan[2], Tianyun Chen[1], and Luqi Huang[1*]

1. State Key Laboratory of Dao-di Herbs Breeding Base, National Resource Center for Chinese Materia Medica, China Academy of Chinese Medical Sciences, Beijing 100700, China.
2. College of animal science and veterinary medicine, Tianjin Agricultural University, Tianjin, 300384, China.

*Address for correspondence
Dr. Chao Jiang (jiangchao0411@126.com); Prof. Luqi Huang (Huangluqi01@126.com)
State Key Laboratory Breeding Base of Dao-di Herbs, National Resource Center for Chinese Materia Medica, China Academy of Chinese Medical Sciences, Beijing, 100700, P.R. China.
Tel: +86 10 64017649
Fax: +86 10 64013996

Running head
New *Ethmostigmus* species from China

Abstract
In this study, we used a combination of morphological and DNA data to delineate *Ethmostigmus* centipedes in China. Two mitochondrial DNA loci (COI and 16S rRNA) and a nuclear DNA locus (28S rRNA) were used to determine the phylogenetic positions of potential species using maximum likelihood and Bayesian inference approaches. On the basis of these analyses, five species of Chinese *Ethmostigmus* are newly recognized: *Ethmostigmus pygomenasoides* Lewis, 1992 **stat. nov.**, and the four new species *E. flavescens* **sp. nov.**, *E. austroyunnanensis* **sp. nov.**, *Ethmostigmus biocolor* **sp. nov.,** and *E. motuoensis* **sp. nov.** These species are described and keyed, and we map their distributions.

Keywords DNA, COI, Taxonomy, Yunnan, Xizang

Introduction

Ethmostigmus Pocock, 1898 is a taxon comprising the largest Otostigminae centipedes, of which 20 valid *Ethmostigmus* species are listed in the Chilobase 2.0 database (Bonato et al. 2016), with distribution ranges extending throughout Africa, India, Southeast Asia, and Australia, including neighbouring islands (Bonato et al. 2016; Joshi & Edgecombe 2019a; Koch & Colless 1986; Lewis 1968; Schileyko & Stoev 2016). Since Attems' global revision of the scolopendromorph centipedes almost 100 years ago (Attems 1930), there have been two large-scale taxonomic studies of this genus and a number of new species have been discovered, Koch (1983) described five novel *Ethmostigmus* species from Australia, and on the basis of an integration of molecular data, morphological, and geographical information, Joshi & Edgecombe (2019a) discovered three new species, namely, *E. agasthyamalaiensis* Joshi & Edgecombe, 2019, *E. sahyadrensis* Joshi & Edgecombe, 2019, and *E. praveen*i Joshi & Edgecombe, 2019 from the Western Ghats of India. Existing literature indicates only a nominate *Ethmostigmus* species and a subspecies of *E. rubripes* (Brandt, 1840) have been recorded to date in China: *Scolopendra rapax* Gervais, 1847 from unspecified localities in China, which is considered synonymous to *E. rubripes rubripes* (Brandt, 1840) by Kraepelin (1903), and *E. rubripes platycephalus* (Newport 1845), which has been noted from the Spratly inseln (=Nansha Islands) (Schileyko & Stagl 2004; Schileyko & Stoev 2016). Apart from these taxa, however, little is known regarding *Ethmostigmus* centipedes inhabiting mainland China.

In this study, we examined some newly discovered *Ethmostigmus* centipedes from Yunnan Province and the Xizang Autonomous Region of mainland China based on a combination of external morphological characters and molecular phylogeny [the mitochondrial DNA loci cytochrome *c* oxidase subunit I (COI) and 16S rRNA (16S) and the nuclear locus 28S rRNA (28S)]. Phylogenetic analysis of the Otostigminae subfamily, performed using DNA sequence data gained in the present and published sequence data retrieved from the GenBank database revealed that at least five *Ethmostigmus* centipede species are distributed throughout mainland China, four of which appear to be new species. A key to the *Ethmostigmus* species found in China is provided.

Material and methods

Specimen collection and identification. Centipede specimens were collected in Yunnan Province and the Xizang Autonomous Region of China during the period from May 2018 to October 2021. During the course of field investigations, we photographed representative individuals using an Olympus E-M10 II camera to document the colouration of living specimens (Fig. 1). Upon collection, all specimens were deposited in 75% ethanol solution. Holotype and paratype specimens have been retained at the Institute of Chinese Materia Medica, China Academy of Chinese Medical Sciences, China (CMMI).

The morphological terminology used in this paper partially follows the standardized terminology (Bonato et al. 2010). Multi-focused montage photographs were obtained using Helicon Focus 6.7.1 software from a sequence of source images acquired using an Olympus SZ16 stereo microscope. Distribution maps were generated using ArcMap 10.7.1 (Fig. 2).

Abbreviations: VL = ventrolateral, VM = ventromedial, M = medial, DM = dorsomedial, CS = corner spine, T = tergite, UL = ultimate leg, and ULBS = ultimate leg-bearing segment.

Phylogenetic sampling and DNA sequence analyses. For the purposes of determining phylogenetic relationships, we selected two mitochondrial loci (16S and COI) and a single nuclear locus (28S). Previously determined *Ethmostigmus* sequences were retrieved from the GenBank database (Table 1). These sequences were augmented by those obtained from the *Ethmostigmus* specimens collected in this study. Genomic DNA was extracted from the legs of these specimens using DNeasy Blood & Tissue Kits (Qiagen, Hilden, Germany), with the isolated DNA being resuspended in 100 µL of buffer and stored at -20°C for subsequent analysis.

The 28S rRNA fragment was amplified using the primer pair 28SF4/28SR5 or Chilo28SF1/Chilo28SR1 (Jiang et al. 2022; Morgan et al. 2002); the 16S rRNA fragment was amplified using the primer pair 16Sar/16Sb (Palumbi et al. 1991; Xiong & Kocher 1991); and COI was amplified using the primer pair LCO1490/HCOoutout or Chilo887F/Chilo887R (Folmer et al., 1994; Jiang et al., 2022; Schwendinger & Giribet 2005). PCR reaction mixtures (total volume 25 µL) contained 12.5 µL of 2× M5 Mix (Transgen, Beijing, China), 0.4 µL each of the forward and reverse primers (10 $\mu mol \cdot L^{-1}$, Sangon, Shanghai, China), and 1 µL (approximately 20 ng) of genomic DNA. Amplification was performed in a Veriti™ thermal cycler (Applied Biosystems, Foster City, CA, USA) using previously described cycling conditions (Jiang et al 2022). For phylogenetic analyses, we adopted Maximum likelihood and Bayesian inference approaches using PhyloSuite (Zhang et al. 2018). Standard statistical tests were applied to evaluate branch support (bootstrap support and posterior probability), and the best-fit substitution models and partitioning strategies were inferred for the combined COI, 16S and 28S dataset using ModelFinder (Kalyaanamoorthy et al. 2017). Based on Akaike Information Criterion assessments, GTR+I+G4 and GTR+G+I were selected as the best-fitting models for maximum likelihood and MrBayes analyses, respectively. Trees for combined dataset were constructed with IQ-TREE (Nguyen et al. 2015) using a maximum likelihood algorithm with 500,000 ultra-fast bootstrap replicates (Minh et al. 2013). Bayesian analyses were performed using MrBayes 3.2.6 (Ronquist et al. 2012) integrated into PhyloSuite with the default settings, and 20,000,000 Markov chain Monte Carlo generations, sampling every 1000 generations. Sequences have been deposited in the GenBank databases with the accessions numbers shown in Table 1.

Results

Taxonomic accounts

Order Scolopendromorpha Pocock, 1895
Family Scolopendridae Newport, 1844

Genus *Ethmostigmus* Pocock, 1898

Diagnosis. Twenty antennal articles, basal four glabrous dorsally. Leg-bearing segment 7 with pair of spiracles. Spiracle on leg-bearing segment 3 enlarged. Forcipular trochanteroprefemoral process absent (or small, without teeth). Coxopleural process bearing apical and lateral spines. Corner spine on ultimate leg prefemur simple.

***Ethmostigmus flavescens* Jiang & Huang sp. nov. 黄筛孔蜈蚣 (**Fig. 1A, Fig. 3)

Material examined.

Holotype. CHINA: Yunnan Province: Mengla county (21.72N, 101.38E), CMMI 20191212003, 12 Dec. 2019, leg. MX. Shi.

Paratypes. CHINA: Yunnan Province: Menghai county, one spm, CMMI 20200628001, 28 Jun. 2020, leg. MX. Shi; **Mengla county:** one spm, Xishuangbanna Tropical Rainforest National Park: Mengyuanxianjing Scenic, 21.7192N, 101.3826E, 680 m a.s.l. CMMI 20200610005, 10 Jun. 2020, leg. JD. Zhang, one spm, CMMI 20190507004, 7 May. 2019, unspecified locality of Mengla county, leg. QY. Ji, 1 spm, CMMI 20191212010, data as for holotype.

Type locality. Yunnan Province: Mengla county.

Etymology. The specific name *flavescens* refers to the yellowish body colour of the new species.

Diagnosis. Forcipular coxosternal tooth-plates with four well-defined teeth on each side, coxopleural process 2.3–2.8 times length of ultimate sternite; with 1–2 apical spines, 0–1 subapical spine, 0–1 dorsal spine, and 1 lateral spine. Ultimate leg prefemur with 2VL, 2VM, 1M, and 2 DM spines.

Holotype description. The colour description is based on photographs of a living specimen (Fig. 1A). Cephalic plate dark yellow, tergites yellow to dark yellow, posterior border of tergites with dark stripes. Antennae and legs pale yellow. Prefemur and femur of ultimate leg dark yellow, whereas tibia and tarsus pale yellow with black stripe on tibia and tarsus 1.

Body length 90 mm. Antennae with 20 articles, basal four articles glabrous dorsally and three ventrally (Fig. 3A, B). Cephalic plate and tergites smooth, with large punctates. Forcipular coxosternal tooth-plates slightly longer than wide, with width-to-length ratio of approximately 1.7:1. Tooth-plates with four well-defined main teeth on each side, the inner two teeth sharing a common base (Fig. 3C). Each tooth with three small lobes; innermost tooth has four or five accessory teeth. The base of tooth-plates defined by oblique sutures diverging at 100°.

Tergites smooth, without hairs or setae. Tergites with complete paramedian sutures from T3 to T20 (Fig. 3E). Complete clearly visible margination beginning from T6. Tergite 21 with parallel lateral margins and width-to-length ratio of 1.5:1 (Fig. 3G). Sternites with complete paramedian sutures starting from S3 (Fig. 3F). The ultimate sternite surface without longitudinal depression, incurved posteriorly, forms a triangle diverging at 115°.

Coxopleural process 2.4–2.8 times length of sternite 21 (Fig. 3H), with one robust apical spine, one subapical dorsal spine distinctly separated from apical spine, one small dorsal spine, and one lateral spine on left (right coxopleural process wounded and showing regeneration, without apical spine and dorsal subapical spine). Pores dense and pore-free area short, extending 40%–45% of length from distal part of coxopleural process to ultimate sternite margin.

All legs with very sparse short setae; first two pairs with two tarsal spurs, and legs 3–20 with one tarsal spur. Leg 1 with one tibial and one femoral spur. Legs 1–20 with two claw spurs. Ultimate legs thick and moderately long (Fig. 3O), with prefemur and femur length ratios of 1.44:1, femur and tibia of 1.3:1, tibia and tarsus 1 of 1.3:1, and tarsus 1 and tarsus 2 of 2.5:1. Ultimate leg without claw spur (Fig. 3N), prefemur with large spines, as follows: 2 VL, 2 VM, 1 M, 2 DM, and 1 corner spine (Fig. 3D, I).

Variation. Details are shown in Table 2. The studied material shows certain variation in the morphology and size of spiracles; in specimen CMMI 20200628001, the spiracle on leg-bearing segment 3 occupies nearly the entire surface of the respective pleuron, whereas the spiracle on leg-bearing segment 7 is large and round. The ultimate legs typically lack claw spurs, although specimens CMMI 20200628001 and CMMI 20190507004 have a single spur on the left leg. Spines on ultimate leg prefemur often have the pattern 2 VL, 2 VM, 1 M, 2 DM, although some specimens were found to have 2 VL, 1 VM, 2 M, and 2 DM spines on one side. The shape and location of the coxopleural process spine are variable. Paratypes CMMI 20200610005 and CMMI 20200628001 have two equal-sized apical spines (Fig. 3P), whereas the holotype has a large apical spine and a smaller subapical spine that is distinctly separated from the apical spine in the process (Fig. 3H).

Distribution. Yunnan (Mengla county, Menghai county). Fig. 2.

Remarks. *Scolopendra rapax* Gervais, 1847 was originally described from a specimen collected in China, the tooth-plates of which are more or less square, with three teeth of which the inner one bears a cusp and the middle one of the three teeth is the largest. *S. rapax* is considered synonymous to *E. rubripes spinosus* (Newport, 1845) (type location: Sri Lanka). *Ethmostigmus flavescens* **sp. nov.** is very similar to *E. rubripes spinosus* with respect body colour and ultimate leg prefemur spine arrangement, although can be distinguished in that the tooth-plates of the former have four distinct teeth on each side, and legs 1–3 to 4 have two tarsal spurs, whereas the latter has three teeth on each side of the tooth-plate, and the two anterior pairs of legs have two tarsal spurs. Joshi and Edgecombe (2018) considered *H. longicauda* (Pocock,1891) from India to be a synonym of *E. rubripes spinosus*, with the former having forcipular coxosternal tooth-plates bearing 3.5 teeth, the innermost being small, and the ultimate leg prefemur bearing 2VL, 1VM, 1M, and 2DM spines.

Ethmostigmus austroyunnanensis **Jiang & Huang sp. nov. 滇南筛孔蜈蚣** (Fig. 1B, Fig. 4A-R)

Material examined.

Holotype. ♂, **CHINA: Yunnan Province: Mangshi:** Menghuan Gold Tower scenic spot: Mts. Leiyarang, 24.4279N, 98.5959E, 1020 m a.s.l., CMMI 20200608081, 08 Jun. 2020, leg. C. Jiang.

Paratypes. CHINA: Yunnan Province: Yingjiang county: 1♂, CMMI 20200610001, Jun. 2020, leg. JD. Zhang, 1♀, CMMI 20190702003, 2 Jul. 2019, leg. JD. Zhang; 1♀, CMMI 20210401105, 5 Apr. 2021, leg. JD. Zhang 1♀; Taiping town, CMMI 20201209104, 9 Dec. 2020, leg. MX. Shi.

Other materials: CHINA: Yunnan Province: Yingjiang county: 3♀♀, Mangyun village, 24.5911N, 97.7723E, CMMI 20190507001–003, 07 May. 2019, leg. QY. Ji; 2♂♂ & 2♀♀, unspecified locality in Yingjiang county, CMMI 20201214112–115, 14 Dec. 2020, leg. QY. Ji; 1♀, unspecified locality in Yingjiang county, CMMI 20190609029, 09 Jun. 2019, leg. JD. Zhang; **Dehong Dai & Jingpo autonomous prefecture:** 1 juvenile, unspecified locality, CMMI 20200319004, 19 Mar. 2020, leg. JZ. Lu.

Type locality. Yunnan Province: Mangshi: Menghuan Gold Tower scenic spots.

Etymology. The specific name *austroyunnanensis* refers to the southern region of Yunnan, the locality in which the new species occurs.

Diagnosis. Forcipular coxosternal tooth-plates with four well-defined teeth on each side, coxopleural process short, approximately 1.6–1.9 times length of sternite 21, with two distinctly separated terminal spines and a lateral spine. Ultimate legs thick and moderately long, with prefemur and femur length ratios of approximately 1.1:1, femur and tibia of 1.3:1, tibia and tarsus 1 of 1.3:1, and tarsus 1 and tarsus 2 of 2.1:1. Ultimate legs prefemur with 3VL, 2VM, 1M, and 2 DM spines. Ultimate leg tibia and tarsus 1 of males swollen.

Holotype description. The colour description is based on photographs of a living specimen (Fig. 1B). Cephalic plate and T1 reddish brown in coloration. Tergites 2 to 21 monochromatic brown. Antennae yellowish. Sternites and legs reddish orange. Leg colour gradually deepens from anterior to posterior legs. Prefemur and femur of ultimate leg jujube red, whereas tibia and tarsus are yellowish. Ultimate leg and leg 20 with black stripe on tibia and tarsus 1.

Body length 93 mm. Posterior margin of cephalic plate underlying T1 (Fig. 4A). Antennae with 20 articles, basal four articles glabrous dorsally and three ventrally (Fig. 4B). Cephalic plate smooth, with large punctates. Forcipular coxosternal tooth-plates slightly longer than wide, with width-to-length ratio of approximately 1.7:1. Tooth-plates with four main teeth on each side (Fig. 4C), which can be divided into two groups, the outermost being smaller than other large teeth, the inner two and outer two teeth sharing respective common bases. Base of tooth-plates defined by oblique sutures diverging at 110°. Article 2 of second maxillary telopodite with spur.

Tergites smooth, without hairs or setae. Tergites with complete paramedian sutures from T3 to T20 (Fig. 4E). Complete clearly visible margination beginning from T6. ULBS tergite slightly curved posteriorly, without median furrow or depression. Tergite 21 with parallel lateral margins and width-to-length ratio of 1.5:1 (Fig. 4I).

Surface of sternite 21 with longitudinal depression, strongly incurved posteriorly, forming a triangle diverging at 120° (Fig. 4J). Coxopleural process 1.8 times length of Sternite 21, with two distinctly separated terminal spines and one lateral spine (Fig. 4J, K). Pores dense and pore-free area narrow, extending 66% of length from distal part of coxopleural process to margin of sternite 21.

Legs 2–20 with very sparse short setae. First two pairs of legs with two tarsal spurs, legs 3–20 with one tarsal spine. Leg 1 with one tibial and one femoral spur. Ultimate legs without setae. Ultimate legs thick and long in male, with prefemur and femur length ratios of 1.1:1, femur and tibia length of 1.34:1, tibia and tarsus 1 length of 1.26:1, and tarsus 1 and tarsus 2 length of 2.05:1. Ultimate leg with two claw spurs (Fig. 4P), prefemur with large spines, as follows: 3 VL, 2 VM, 1 M, 2 DM spines, and 1 corner spine (Fig. 4D, H).

Variation. Details are shown in Table 2. Body length up to 120 mm (paratype CMMI 20210401105). The ultimate leg shows sexual dimorphism, with the tibia and tarsus 1 prominently swollen in males (holotype, Fig. 4Q) and slender in females (paratype CMMI 20201209104, Fig. 4R).

Distribution. Yunnan (Dehong Dai and Jingpo Autonomous Prefecture). Fig. 2.
Remarks: *Ethmostigmus austroyunnanensis* **sp. nov.** shows pronounced sexual dimorphism in the ultimate leg, with the tibia and tarsus 1 being more prominently swollen in males than in females. Mating observations have indicated that specimens with swollen tarsi can spin webs and produce spermatophores and are accordingly sexed as male, whereas specimens lacking swollen tarsi and receiving spermatophores can be sexed as female. To the best of our knowledge, sexual dimorphism in the genus *Ethmostigmus* Pocock, 1898 is described here for the first time.

***Ethmostigmus biocolor* Jiang & Huang sp. nov.** 二色筛孔蜈蚣 **(**Fig. 1C, Fig. 5)
Material examined.
Holotype. CHINA: Yunnan Province: Yingjiang county (24.59N, 97.77E**)**, CMMI 20200610002, Jun. 2020, leg. JD. Zhang.
Paratypes. CHINA: Yunnan Province: Yingjiang county: one spm, Mangyun village, 24.5911N, 97.7723E, CMMI 20191212007, 12 Dec. 2019, leg. MX. Shi; two spms, unspecified locality in Yingjiang county, CMMI 20201209102–103, 09 Dec. 2020, leg. MX. Shi.
Other materials: CHINA: Yunnan Province: Yingjiang county: one spm, CMMI 20200610003, Jun. 2020, leg. JD. Zhang; two spms, CMMI 20190712109–110, Jul. 2019, leg. MX. Shi; one spm, CMMI 20201209101, 9 Dec. 2020, leg. MX. Shi.
Type locality. Yunnan Province: Yingjiang county.
Etymology. The specific name *biocolor* refers to the strong contrast in colouration of the body and locomotory legs.
Diagnosis. Forcipular coxosternal tooth-plates with four well-defined teeth on each side. Forcipule bearing small rudimentary forcipular trochanteroprefemoral process. with low median keel from T6 to T20. Coxopleural process approximately 2.5 times length of sternite 21, with one apical spine, one subapical spine, and one lateral spine. Ultimate leg prefemur with 3VL, 1–2VM, 1–2M, and 2DM spines.
Holotype description. The colour description is based on photographs of a living specimen. Cephalic plate, antennae, tergites, and ultimate leg monochromatic blue-violet. Sternites orange. Legs, except ultimate leg prefemur, orange-red; femur, tibia,

and tarsus 1 blue; tarsus 2 pale yellow.

Body length 90 mm. Posterior margin of cephalic plate underlying T1 (Fig. 5A). Antennae with 20 articles, basal four articles glabrous dorsally and three ventrally (Fig. 5B). Cephalic plate smooth, with large punctates. Forcipular coxosternal tooth-plates slightly longer than wide, with four well-defined main teeth on each side, and width-to-length ratio of approximately 1.36:1. Each tooth bearing small lobes, except outermost. Tooth-plate base defined by oblique sutures diverging at 100°. Article 2 of second maxillary telopodite with spur. Forcipule base with toothless rudimentary trochanteroprefemoral process (Fig. 5C).

Tergites weakly corrugated, with complete low rounded median keel from T6 to T20 (Fig. 5E), and incomplete in T21 (Fig. 5G). Tergites without hairs or setae. Complete clearly visible margination beginning from T6. ULBS tergite slightly curved posteriorly, without median furrow or depression. ULBS width-to-length ratio of 1.6:1 (Fig. 5G).

Surface of sternites smooth. Sternites with complete paramedian sutures starting from S3 (Fig. 5F). Sternite 21 surface with longitudinal depression that is strongly incurved posteriorly and forms a triangle that diverges at 95° (Fig. 5H). Coxopleural process 2.5 times length of sternite 21, with one apical spine, one dorsal subapical spine distinctly separated from apical spine, and one lateral spine (Fig. 5P). Pores dense and pore-free area narrow, extending 75%–80% of length from distal part of coxopleural process to margin of sternite 21.

All legs have very sparse short setae. All legs, including the ultimate leg, with two claw spurs. Leg 1 with two tarsal spurs, legs 2–20 with one tarsal spur. Leg 1 with one tibial and one femoral spur. Ultimate legs long and slender, with prefemur and femur length ratio of 1.05:1, femur and tibia of 1.25:1, tibia and tarsus 1 of 1.20:1, and tarsus 1 and tarsus 2 of 2.05:1. Ultimate leg prefemur with large spines, as follows: 3 VL, 1 VM, 2 M, 2 DM spines, and 1 corner spine on left prefemur (Fig. 5D, I), and 3 VL, 1 VM, 1 M, 1 DM spines, and 1 corner spine on right prefemur (to be interpreted as regeneration).

Variation. Details are shown in Table 2. Body length up to 108 mm (paratype CMMI 20201209102). The spine on the ultimate leg prefemur often with 3 VL, 2 VM, 2 M, and 2 DM spines, but specimen CMMI 20200712109 with 3 VL, 1 VM, 2 M, and 2 DM spines and specimen CMMI 20200712109 with 4 VL spines on left leg prefemur.

Distribution. Yunnan (Yingjiang county). Fig. 2.

Remarks. The trochanteroprefemoral process is deemed to be a plesiomorphic character that is shared within *Rhysida*, and considered the major characteristic distinguishing *Rhysida* from *Ethmostigmus*. Pocock (1891) described the amonotypic species *Ethmophorus monticola* as having four glabrous antennal articles and the presence of a forcipular trochanteroprefemoral process. Kraepelin (1903) transferred this species to *Rhysida*, which has a number of characters in common with *Ethmostigmus*, including a large spiracle on segment 3, robust forcipules, an elongated coxopleural process, and four glabrous basal antennal articles (Joshi et al. 2019). The presence of a trochanteroprefemoral process-like structure in *Ethmostigmus biocolor* **sp. nov.** limits its utility as a critical character separating *Rhysida* and *Ethmostigmus*.

Ethmostigmus motuoensis **Jiang & Huang sp. nov. 墨脱筛孔蜈蚣** (Fig. 1D, Fig. 6)

Material examined.

Holotype. CHINA: Xizang Autonomous Region: Motuo county (29.48N, 96.09E), CMMI 20211008105, 08 Oct. 2021, leg. SY. Zhao.

Paratypes. CHINA: Xizang Autonomous Region: Motuo county, one spm, CMMI 20200511001, 11 May. 2020, leg. MX. Shi; two spms, CMMI 20210316107–108, Mar. 2021, leg. MX. Shi; one spm, CMMI 20190712112, Jul. 2019, leg. MX. Shi.

Type locality. Xizang Autonomous Region: Motuo county.

Etymology. The specific name *motuonesis* refers to Motuo county, the locality in which the new species occurs.

Diagnosis. Forcipular coxosternal tooth-plates with four well-defined teeth on each side. Forcipules with small rudimentary forcipular trochanteroprefemoral process. Tergite with low median keel from T6 to T20. Coxopleural process approximately three times length of sternite 21, with one apical spine, one subapical spine, one dorsal spine, and one lateral spine. Ultimate leg prefemur with 3VL, 2VM, 2M, and 2DM spines.

Description. The colour description is based on photographs of a living specimen. Colouration of cephalic plate and T1 jujube red. Antennae and T2 to T21 reddish-brown in colour. Prefemur and femur of legs 1 to 19 orange red; tibia and tarsus 1 blue, gradually deepening in colour from anterior to posterior legs, tarsus 2 pale yellow. Leg 20 prefemur orange red; femur, tibia and tarsus 1 blue, tarsus 2 pale yellow. Ultimate leg prefemur jujube red; femur, tibia, and tarsus deep blue.

Body length 90 mm. Posterior margin of cephalic plate underlying T1 (Fig. 6A). Antennae with 20 articles, basal four articles glabrous dorsally and three ventrally (Fig. 6B). Cephalic plate smooth with large punctates. Forcipular coxosternal tooth-plates slightly longer than wide, with four well-defined main teeth on each side, and width-to-length ratio of approximately 1.46:1. Each tooth bearing indistinct small lobes, except outermost. Tooth-plate bases defined by oblique sutures diverging at 110°. Article 2 of second maxillary telopodite with spur. Forcipule base with toothless rudimentary trochanteroprefemoral process (Fig. 6C).

Tergites weakly corrugated, with complete low rounded median keel from T7 to T20 (Fig. 6E), although incomplete in T21 (Fig. 6G). Tergites without hairs or setae; complete paramedian sutures from T4 to T20. Complete clearly visible margination beginning from T4. ULBS tergites slightly curved posteriorly, without median furrow or depression. ULBS tergite width-to-length ratio of 1.6:1.

Surface of sternites smooth. Sternite paramedian sutures incomplete, covering 50%–80% of sternite length, and beginning at sternite 3 (Fig. 6F). Sternite 21 surface with deep longitudinal depression that is incurved posteriorly and forms a triangle that diverges at 125°. Coxopleural process incurved posteriorly, three times length of sternite 21 (Fig. 6H), with one robust apical spine, one dorsal subapical spine distinctly separated from apical spine, one small dorsal spine, and one lateral spine (Fig. 6P). Pores dense and pore-free area narrow, extending 85%–90% length from distal part of coxopleural process to margin of sternite 21.

All legs with very sparse short setae. Legs 1–20 have two claw spurs. Leg 1 with two tarsal spurs, legs 2–20 with one tarsal spur. Leg 1 with one tibial and one femoral spur. Ultimate legs long and slender, with prefemur and femur ratio of 1.35:1, femur and tibia of 1.11:1, tibia and tarsus 1 of 1.30:1; tarsus 1 and tarsus 2 of 2.17:1. Ultimate leg without claw spur (Fig. 6N), prefemur with large spines, as follows: 3 VL, 2 VM, 2 M, 2 DM spines, and 1 corner spine (Fig. 6D, I).

Variation. Details are shown in Table 2. Body length up to 110 mm (paratype CMMI 20200511001). The spine on the ultimate leg prefemur often with 3 VL, 2 VM, 2 M, and 2 DM spines, but paratype CMMI 20210316108 with three VM spines. The spines of the coxopleural process are variable, with two lateral spines on paratype CMMI 20190712112 and no dorsal spine on the right process. The length of sternite 21 of paratype CMMI 20190712112 is noticeably longer than that of other specimens, giving a coxopleural process to sternite 21 length ratio of 2.7:1.

Distribution. Xizang (Motuo county). Fig. 2.

Remarks. This species is similar to *E. biocolor* **sp. nov.** with respect to the complete median keels on tergites and forcipule bearing a small rudimentary trochanteroprefemoral process, although differs in terms of the coxopleural process, which is clearly longer (~three times the length of sternite 21) and bears a dorsal spine, whereas in *E. biocolor* **sp. nov.,** the coxopleural process is approximately 2.5 times the length of sternite 21, and lacks a dorsal spine. Haase (1887) described the species *Heterostoma rapax silhetense* from Silhet (India), which is also synonymous to *E. pygomegas* (Kohlrausch, 1879) from the Himalayas, the coxopleural process of which lacks a dorsal spine and the prefemur of the ultimate leg often has 3 VL, 2 VM, 2 M, and 2 DM spines, similar to *E. biocolor* **sp. nov.** However, both *E. pygomegas* (Kohlrausch, 1879) and *H. rapax silhetens* (Haase, 1887) lack complete median keels and a rudimentary trochanteroprefemoral process. Consequently, we consider both *E. biocolor* **sp. nov.** and *Ethmostigmus motuonesis* **sp. nov.** to be new species.

***Ethmostigmus pygomenasoides* Lewis, 1992 stat. nov. 斑足筛孔蜈蚣 (**Fig. 1E, Fig. 7)

Ethmostigmus trigonopodus pygomenasoides Lewis, 1992: 449-450, Fig. 45-51, 53-54.

Type locality. Nepal: Myagdi.

Holotype. Specimen 7 (SMF 6455), 87 mm, **NEPAL**: **Myagdi Distr.**: near Pelma, 2650–2700 m, 29 May 1973, leg. J. Martens. (based on Lewis, 1992)

Material examined. CHINA: Xizang Autonomous Region: Jilong county: Jilonggou: one spm, CMMI 20200905127, 05 Sept. 2020, leg. JD. Zhang.

Diagnosis. Forcipular coxosternal tooth-plates with four well-defined teeth on each side, coxopleural process approximately two times length of sternite 21, terminally two-spined, one to four dorsal spines, and one lateral spine. Ultimate leg prefemur with 2–3VL, 1–2VM, 1–2M, and 1–2 DM spines.

Description of Chinese specimen. The colour description is based on photographs of a living specimen (Fig. 1E). Cephalic plate, antennae, and tergites monochromatic olive yellow. Legs 1 to 20 pale yellow, with black stripes on femur, tibia, and tarsus, the size and color of which gradually deepen from anterior to posterior legs. Ultimate leg prefemur orange; femur, tibia, and tarsus pale yellow with light black stripes.

Body length 73 mm. Posterior margin of the cephalic plate underlying T1 (Fig. 7A). Antennae with 20 articles, basal four articles glabrous dorsally and three ventrally (Fig. 7B). Cephalic plate smooth, with large punctures. Forcipular coxosternal tooth-plates slightly longer than wide, with four main teeth on each side; width-to-length ratio of left and right tooth-plates approximately 1.40:1 and 1.57:1, respectively (Fig. 7C). Innermost tooth has two or three accessory teeth. Base of tooth-plates defined by oblique sutures diverging at 110°. Second maxillary claw with two accessory spines. Article 2 of second maxillary telopodite with several long setae.

Surface of tergites smooth and sparsely punctate with visible setae. Tergites 3 to 20 with complete paramedian sutures (Fig. 7E). Complete clearly visible margination beginning from T5 or T6. Tergite of ULBS slightly curved posteriorly, without median furrow or depression (Fig. 7G). T21 width-to-length ratio of 1.32:1.

Sternites with complete paramedian sutures starting from S3. Sternite 21 incurved posteriorly, forming triangle diverging at 120° with weak longitudinal depression (Fig. 7H). Coxopleural process 2.03 times length of sternite 21, with two distinctly separated terminal spines, three dorsal spines distant from terminal spines, and one lateral spine (Fig. 7P). Pores dense and pore-free area narrow, extending approximately 80% of length from distal part of coxopleural process to margin of sternite 21.

Legs with very short setae. All legs, including the ultimate leg, with two claw spurs. Leg 1 with one tibial spur and two tarsal spurs, without prefemoral and femoral spurs, and legs 2–20 with one tarsal spur. Leg 1 with one tibial and one femoral spur. Ultimate legs moderately long, prefemur and femur length ratios of 1.29:1, femur and tibia of 1.17:1, tibia and tarsus 1 of 1.32:1, and tarsus 1 and tarsus 2 of 1.95:1. Prefemur with large spines, as follows: 3 VL, 2 VM, 2 M, 2 DM spines, and 1 corner spine (Fig. 7D, I).

Distribution. Xizang (Jilong county) (Fig. 2); Nepal (Myagdi, Lalirpur, Taplejung, Gorkha).

Remarks. In their examination of five specimens of *E. trigonopodus* from West Nepal and three specimens from Central Nepal, Schileyko and Stagl (2004) found that these showed no distinct differences from typical representatives of the nominative form. However, the findings of molecular phylogeny analyses indicated that *E. pygomenasoides* and *E. austroyunnanensis* **sp. nov.** are reciprocally monophyletic and grouped with *E. trigonopodus* from Africa with relatively moderate node support (See blew), and thereby elevating the former to full specific status as *E. pygomenasoides* Lewis, 1992 **stat. nov**. *E. trigonopodus* from West Nepal needs to be re-examined and compared with African specimens to ascertain whether these specimens are *E. trigonopodus* or *E. pygomenasoides*. The original description by Lewis (1992) states that *E. pygomenasoides* is characterized by an ultimate leg prefemur bearing three rows of spines of 2–3 VL, 1–2 VM, and 1–2 DM, and a simple corner spine. However, Fig. 54 shown in this paper clearly indicates four rows of spines of 3 VL, 2VM, 2M, and 1 DM spine, which resemble the pattern observed in Chinese specimens. Furthermore, the specimens of *E. pygomenasoides* from Nepal generally lack small tooth lobes, whereas the Chinese specimens examined in the present study are characterized by inner teeth bearing accessory teeth. Accordingly, further data will be necessary to clarify the range of variation in this species and distinguish it from another Himalayan species, *E. pygomegas* (Kohlrausch, 1879).

Molecular phylogenetic analysis. The COI, 16S rRNA, and 28S rRNA loci of *Ethmostigmus* species analysed in this study were sequenced and aligned with sequences obtained for taxa in other major lineages of Otostigminae, including *Alluropus*, *Alipes*, *Digitipes*, *Edentistoma*, *Otostigmus*, and *Rhysida*, with *Scolopendra mutilans* Koch, 1878 being selected as an outgroup. We accordingly obtained a final alignment dataset of 1299 base pairs (bp) of sequencing data, comprising 531, 455, and 314 bp of COI, 16S, and 28S, respectively. Phylogenetic analysis was conducted based on maximum likelihood and Bayesian approaches, which indicated that *Ethmostigmus* is a monophyletic taxon with likelihood bootstrap (BS) support of 95% and posterior probability (PP) of 1.00. The genus *Ethmostigmus* is divided into the following three species groups: the *trigonopodus-pygomegas* group (clade A) comprising the African species *E. trigonopodus*, and the five China *Ethmostigmus* species E. *austroyunnanensis* **sp. nov.**, *E. biocolor* **sp. nov.**, *E. metuoensis* **sp. nov.**, *E. flavescens* **sp. nov.** and *E. pygomenasoides* Lewis, 1992, with a PP of 1.00 and BS of 87%; the *rubripes* group (clade B) comprising the two Australian species *E. rubripes* and *E. curtipes*; and the *tristis* group (clade C) comprising the five Indian Peninsula species *E. coonooranus* Chamberlin, 1920, *E. tristis* (Meinert, 1886), *E. agasthyamalaiensis* Joshi & Edgecombe, 2019, *E. sahyadrensis* Joshi & Edgecombe, 2019, and *E. praveeni* Joshi & Edgecombe, 2019a, and a Sri Lanka species (*E. rubripes spinosus*) with PP of 0.91 and BS of 88% (Fig. 8). The distinct status of these three groups is also supported morphologically with respect to tooth plate characteristics, with the for *rubripes*, *tristis*, and *trigonopodus-pygomegas* groups being distinguished by 3, 3.5 (the innermost bearing a cusp), and 4 main teeth on each tooth-plate, respectively.

All five *Ethmostigmus* species collected in China belong to the *trigonopodus-pygomegas* group and comprise three clades in the molecular phylogeny. One has moderately high support (PP = 1.00, BS = 94%) for the reciprocally monophyletic Xizang species pair *E. biocolor* **sp. nov.** and *E. metuoensis* **sp. nov.**, the monophyly of each of which is also strongly supported (PP = 1.00, BS = 100%). The remaining two clades include two Yunnan species and one Xizang species, *E. flavescens* **sp. nov.**, is sister to *E. austroyunnanensis* **sp. nov.**, and *E. pygomenasoides* (PP = 0.9, BS = 85%). With moderate node support (PP = 0.9), *E. austroyunnanensis* **sp. nov.** is considered a sister to *E. pygomenasoides* and grouped to *E. trigonopodus*.

Discussion

According to Conservation International (conservation.org), there are 36 biodiversity hotspots distributed worldwide (Kellee, 2016)., and notably all five *Ethmostignus* species identified on mainland China have been discovered in biodiversity hotspot regions: *E. flavescens* **sp. nov.**, *E. austroyunnanensis* **sp. nov.**, and *E. biocolor* **sp. nov.** from the Indo-Burma hotspot region, and *E. pygomenasoides* and

E. motuoensis **sp. nov.** from the Himalayas. These species belong to a monophyletic group that is sister to Australian and Peninsular Indian species. Since divergence estimates and biogeographic studies of *Ethmostigmus*, Joshi and Edgecombe (2019b) have proposed that the early evolutionary history of the genus *Ethmostigmus* was driven by the Gondwanan break-up. They suggest that *Ethmostigmus* has a Gondwanan origin and has subsequently undergone independent radiation in Peninsular India and Australia. For the Africa-wide species *E. trigonopodus* (Leach, 1817), which is nested in the *trigonopodus-pygomegas* group and is sister to *E. austroyunnanensis* **sp. nov.** from Southwest China, it is more likely that *Ethmostigmus* in China evolved via dispersal/vicariance from Australasia and radiative evolution in the Indo-Burma biodiversity hotspot. However, to evaluate the potential evolutionary scenarios for *trigonopodus-pygomegas* group species in these locations, extensive taxon sampling across Southeast Asia (e.g. Myanmar and Thailand), East India, the Andaman and Nicobar Islands, and Sri Lanka is required.

We found that several of the external morphological features often used to identify *Ethmostigmus* differ significantly among the *Ethmostigmus* specimens collected in China. Consequently, distinguishing inherent variance across specimens from variation attributable to damage or regeneration represents a notable challenge, particularly with respect to the form and arrangement of spines on the ultimate legs or the coxopleural process. Accordingly, it is difficult to eliminate cryptic *Ethmostigmus* species in China and neighbouring regions solely based on the morphological characters of Chinese *Ethmostigmus* dispersed in biodiversity hotspots. This problem is highlighted by the Nepalese specimens of *E. pygomenasoides* initially described by Lewis (1992), which were found to show high variability in the number of spines on the ultimate legs (totaling 7–10 spines in 3 or 4 rows) and variable dorsal spines (1–4) on the coxopleural process. Moreover, these characteristics overlap to varying extents with those of the sympatric species, *E. pygomegas*, which frequently has four rows of spines arranged in rows of 3, 2, 1–2, 2 on the ultimate leg (Fig. 9), whereas a syntype (NHMW MY1561) has four rows spines arranged in rows of 2, 2, 1, 2 on the ultimate leg (Fig. 10). Given this ambiguity, further data are required to evaluate the genetic variation among specimens and to determine whether the current taxonomic designations are attributable to misidentification or whether cryptic *Ethmostigmus* species exist.

Key to the *Ethmostigmus* species of China

1. With three main teeth on each side of tooth-plates..2
– With four main teeth on each side of tooth-plates..3
2. Coxopleural process 2.6–3.2 times length of sternite 21...*E. rubripes platycephalus*
– Coxopleural process 1.6–2 times length of sternite 21.................*E. rubripes rubripes*
3. Coxopleural process 1.5–2.3 times length of sternite 21, coxopleural process with 2 apical spines..4
– Coxopleural process 1.3–3.3 times length of sternite 21, coxopleural process with 1 apical spine..5
4. Coxopleural process without dorsal spine, male ultimate leg tibia and tarsus 1 more

swollen than in female..*E. austroyunnanensis* **sp. nov.**
– Coxopleural process without 1–4 dorsal spines..............*E. pygomenasoides* **stat. nov.**
5. Two VL spines on ultimate leg prefemur..................................*E. flavescens* **sp. nov.**
– Three VL spines on ultimate leg prefemur...6
6. Coxopleural process 2.2–2.7 times length of sternite 21, coxopleural process with dorsal spine...*E. motuoensis* **sp. nov.**
– Coxopleural process 2.7–3.3 times length of sternite 21, coxopleural process without dorsal spine...*E. biocolor* **sp. nov.**

Acknowledgements
We sincerely thank Ji Quanyu (Hebei University, China), and Shi Mengxuan (Henan University, China), Zhang Junduo (Tsinghua University, China) for contributing materials to this study. We are very grateful to Nadine Dupérré (Zoological Museum Hamburg (ZMH), Germany), Oliver Macek (Naturhistorisches Museum Wien (NHMW), Austria), Nesrine Akkari (NHMW, Austria), and Gregory D. Edgecombe (Natural History Museum (NHML), UK), who kindly help to provided photographs of type materials of *E. pygomegas* (Kohlrausch, 1879). This work was supported by National Natural Science Foundation of China (82073972), the Fundamental Research Funds for the Central public welfare research institutes (ZZXT2021011) and the fund of Ability Establishment of Sustainable Use for Valuable Chinese Medicine Resources (2060302). Collections were made under the permit of the Fourth National Survey Chinese Material Medical Resources.

References
Attems C. (1930) Myriapoda 2. Scolopendromorpha. Schulze, F.E. & Kükenthal W. (Eds.), Das Tierreich, Berlin: 308 pp. https://doi.org/10.1515/9783112373002
Bonato L, Chagas Junior A, Edgecombe GD, Lewis JGE, Minelli A, Pereira LA, Shelley RM, Stoev P, Zapparoli M. (2016) ChiloBase 2.0 - A World Catalogue of Centipedes (Chilopoda). Available at https://chilobase.biologia.unipd.it, [Accessed 19/04/2022].
Bonato L, Edgecombe GD, Lewis JGE, Minelli A, Pereira LA, Shelley RM, Zapparoli M (2010) A common terminology for the external anatomy of centipedes (Chilopoda). ZooKeys 69: 17–51. https://doi.org/10.3897/zookeys.69.737
Folmer O, Black M, Hoeh W, Lutz R, Vrijenhoek R (1994) DNA primers for amplification of mitochondrial cytochrome c oxidase subunit I from diverse metazoan invertebrates. Molecular Marine Biology and Biotechnology 3: 294–299.
Haase E. (1887). Die Indisch-Australischen Myriopoden. Pt. I. Chilopoden - Abhandlungen und Berichte des Königlichen Zoologischen und. Anthropologisch-Ethnographischen Museums zu Dresden, 5: 1–118.
Jiang C, Bai Y, Shi MX, Liu J (2020) Rediscovery and phylogenetic relationships of the scolopendromorph centipede *Mimops orientalis* Kraepelin, 1903 (Chilopoda): a monotypic species of Mimopidae endemic to China, for more than one century. Zookeys 932: 75–91. https://doi.org/10.3897/zookeys.932.51461

Jiang C, Liu J, Zhang J, Huang L (2022) Integrative taxonomy reveals a new *Scolopendra* species (Chilopoda: Scolopendromorpha: Scolopendridae) from China. Zootaxa, Under review.

Joshi J, Karanth KP (2011) Cretaceous–Tertiary diversification among select scolopendrid centipedes of South India. Molecular Phylogenetics and Evolution, 60(3): 287–294. https://doi.org/10.1016/j.ympev.2011.04.024

Joshi J, Edgecombe GD (2019a) Molecular phylogeny and systematics of the centipede genus *Ethmostigmus* Pocock (Chilopoda: Scolopendromorpha) from peninsular India. Invertebrate Systematics 32(6): 1316–1335. https://doi.org/10.1071/is18030

Joshi J, Edgecombe GD (2019b) Evolutionary biogeography of the centipede genus *Ethmostigmus* from Peninsular India: testing an ancient vicariance hypothesis for Old World tropical diversity. BMC Evolutionary Biology 19: 41. https://doi.org/10.1186/s12862-019-1367-6

Joshi J, Karanth PK, Edgecombe GD (2020) The out-of-India hypothesis: evidence from an ancient centipede genus, *Rhysida* (Chilopoda: Scolopendromorpha) from the Oriental Region, and systematics of Indian species. Zoological Journal of the Linnean Society 189(3): 828–861. https://doi.org/10.1093/zoolinnean/zlz138

Kalyaanamoorthy S, Minh BQ, Wong TK, Von Haeseler A, Jermiin LS (2017) ModelFinder: fast model selection for accurate phylogenetic estimates. Nature Methods 14(6): 587–589. https://doi.org/10.1038/nmeth.4285

Kellee K (2016) Biodiversity Hotspots Map (English labels) (2016.1). Zenodo. https://doi.org/10.5281/zenodo.4311850

Kraepelin K (1903): Revision der Scolopendriden. - Mitteilungen aus dem Naturhistorischen Museum in Hamburg 20: 1-276

Koch LE (1983) A taxonomic study of the centipede genus *Ethmostigmus* Pocock (Chilopoda: Scolopendridae: Otostigminae) in Australia. Australian Journal of Zoology 31(5): 835–849. https://doi.org/10.1071/zo9830835

Koch LE, Colless DH (1986) Numerical Taxonomy of Australian Species of 9 Genera of Scolopendrid Centipedes (Chilopoda, Scolopendridae). Australian Journal of Zoology 34(1): 87–105. https://doi.org/10.1071/zo9860087

Kohlrausch, E. (1879) Beiträge zur Kenntniss der Scolopendriden. Journal des Museum Godeffroy, 14, 51–74.

Lewis JGE (1968) On the identity of the African centipedes *Ethmostigmus australianus stechowi* Verhoeff and *Pseudocryptops walkeri* Pocock (Chilopoda: Scolopendromorpha). Journal of Natural History 2(2): 173–176. https://doi.org/10.1080/00222936800770781

Lewis JGE (1992) Scolopendrid centipedes from Nepal and Kashmir (Chilopoda: Scolopendromorpha). Senckenbergiana Biologica 72(4/6): 435–456.

Minh BQ, Nguyen MAT, von Haeseler A (2013) Ultrafast approximation for phylogenetic bootstrap. Molecular Biology and Evolution 30(5): 1188–1195. https://doi.org/10.1093/molbev/mst024

Morgan JA, DeJong RJ, Jung Y, Khallaayoune K, Kock S, Mkoji GM, Loker ES (2002) A phylogeny of planorbid snails, with implications for the evolution of Schistosoma parasites. Molecular Phylogenetics and Evolution 25(3): 477–488. https://doi.org/10.1016/s1055-7903(02)00280-4

Nguyen LT, Schmidt HA, Von Haeseler A, Minh BQ (2015) IQ-TREE: a fast and effective stochastic algorithm for estimating maximum-likelihood phylogenies. Molecular Biology and Evolution 32(1): 268–274. https://doi.org/10.1093/molbev/msu300

Palumbi SR, Martin A, Romano S, McMillan WO, Stice L, Grabowski G (1991) The simple fool's guide to PCR. Department of Zoology Special Publication, University of Hawaii, Honolulu, HI.

Ronquist F, Teslenko M, van der Mark P, Ayres DL, Darling A, Höhna S, Larget B, Liu L, Suchard MA, Huelsenbeck JP (2012) MrBayes 3.2: efficient Bayesian phylogenetic inference and model choice across a large model space. System Biology 61: 539–542. https:// doi.org/10.1093/sysbio/sys029

Schileyko AA, Stagl V (2004) The collection of scolopendromorph centipedes (Chilopoda) in the Natural History Museum in Vienna: a critical re-evaluation of former taxonomic identifications. Annalen des Naturhistorischen Museums in Wien. Serie B für Botanik und Zoologie 105B: 67–137.

Schileyko AA, Stoev PE (2016) Scolopendromorpha of New Guinea and adjacent islands (Myriapoda, Chilopoda). Zootaxa 4147(3): 247–280. https://doi.org/10.11646/zootaxa.4147.3.3

Schwendinger P, Giribet G (2005) The systematics of south–east Asian genus *Fangensis* Rambla (Opiliones: Cyphophthalmi: Stylocellidae). Invertebrate Systematics 19: 297–323. https://doi.org/10.1071/is05023

Systematic revision and phylogenetic reassessment of the centipede genera *Rhysida* Wood, 1862 and *Alluropus* Silvestri, 1912 (Chilopoda: Scolopendromorpha) in Southeast Asia, with further discussion of the subfamily Otostigminae. Invertebrate Systematics, 32(5), 1005–1049. http://dx.doi.org/10.1071/IS17081

Pocock RI (1891) Notes on the synonymy of some species of Scolopendridae with descriptions of new genera and species of the group. Annals and Magazine of Natural History, (6)7: 51–68. https://doi.org/10.1080/00222939109460577

Thofern D, Duperre N, Harms D (2021) An annotated type catalogue of the centipedes (Myriapoda: Chilopoda) held in the Zoological Museum Hamburg. Zootaxa 4977(1): 1–103. https://doi.org/10.11646/zootaxa.4977.1.1

Vahtera V, Edgecombe GD, Giribet G (2012) Evolution of blindness in scolopendromorph centipedes (Chilopoda: Scolopendromorpha): insight from an expanded sampling of molecular data. Cladistics 28 (1): 4–20. https://doi.org/10.1111/j.1096-0031.2011.00361.x

Vahtera V, Edgecombe GD, Giribet G (2013) Phylogenetics of scolopendromorph centipedes: can denser taxon sampling improve an artificial classification? Invertebrate Systematics 27(5): 578–602. https://doi.org/10.1071/IS13035

Vahtera V, & Edgecombe GD (2014) First molecular data and the phylogenetic position of the millipede-like centipede *Edentistoma octosulcatum* Tömösvary, 1882 (Chilopoda: Scolopendromorpha: Scolopendridae). PLoS One 9(11): e112461. https://doi.org/10.1371/journal.pone.0112461

Xiong B Kocher TD (1991) Comparison of mitochondrial DNA sequences of seven morphospecies of black flies (Diptera: Simuliidae). Genome 34: 306–311. https://doi.org/10.1139/g91-050

Zhang D, Gao F, Jakovlić I, Zou H, Zhang J, Li WX, Wang GT (2020) PhyloSuite: an integrated and scalable desktop platform for streamlined molecular sequence data management and evolutionary phylogenetics studies. Molecular Ecology Resources 20(1): 348–355. https://doi.org/10.1111/1755-0998.13096

Figure legends

Figure 1. Habitus of *Ethmostigmus* from China. (A) *E. flavescens* **sp. nov.**; (B) and (C) *E. austroyunnanensis* **sp. nov.**; (D) *E. biocolor* **sp. nov.**; (E) *E. motuoensis* **sp. nov.**; (F) *E. pygomenasoides* Lewis, 1992 **stat. nov.**

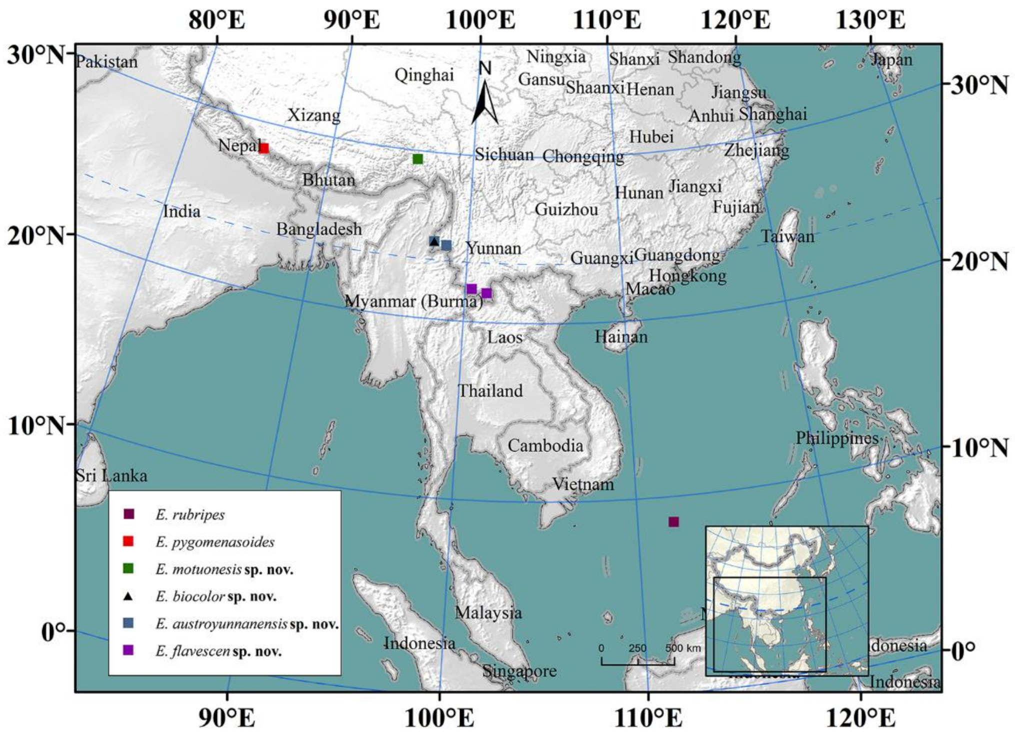

Figure 2. Distribution of *Ethmostigmus* in China.

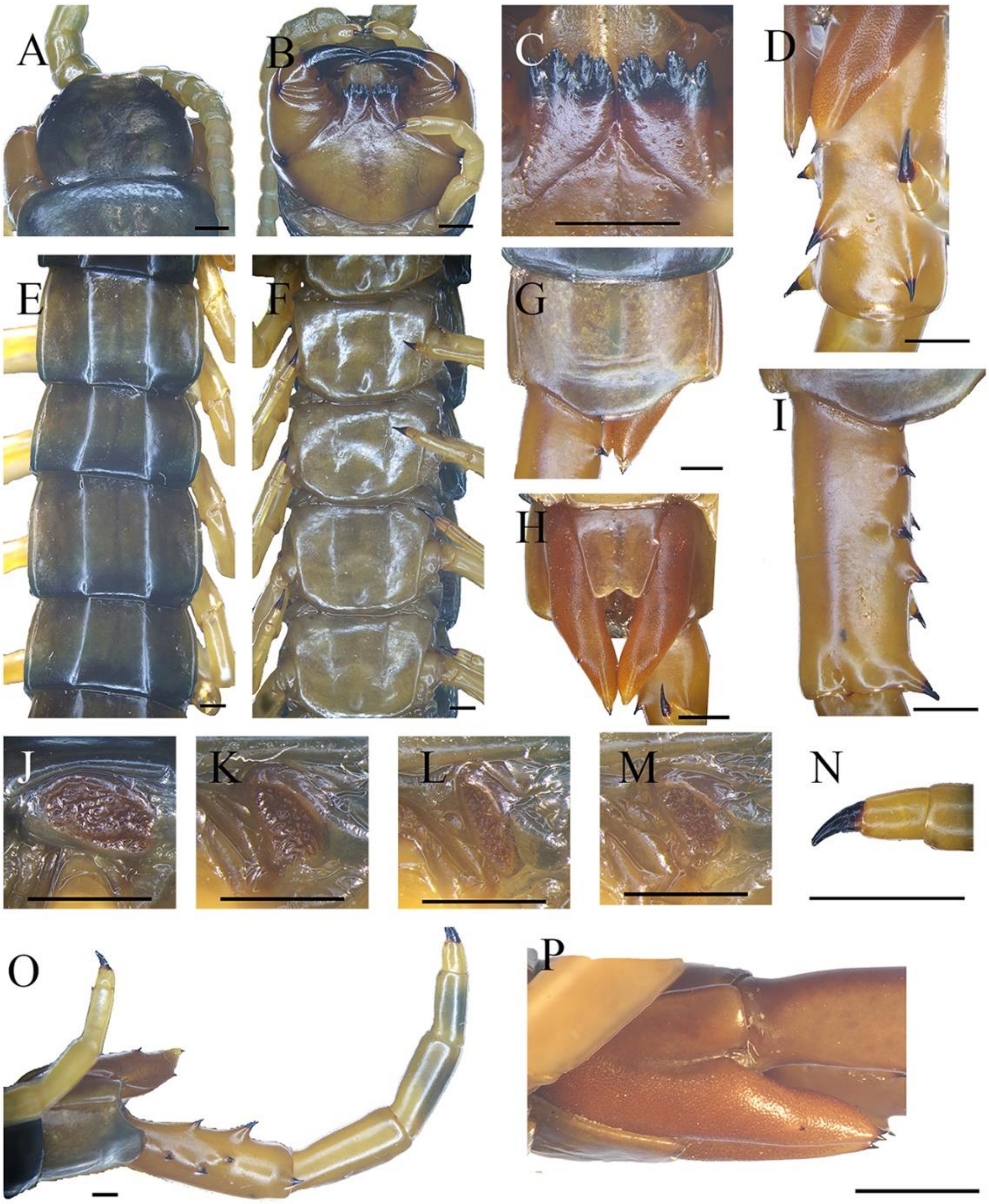

Figure 3. *Ethmostigmus flavescens* **sp. nov.** (A)–(O) holotype CMMI 20200608081. (A) Cephalic plate, T1 tergite, and proximal part of antennae, dorsal view; (B) cephalic plate and proximal part of antennae, ventral view, (C) tooth-plates, ventral view; (D) ultimate leg prefemur, lateral view; (E) tergites 9–12; (F) sternites 9–12; (G) tergite of the ultimate leg-bearing segment (ULBS), dorsal view; (H) coxopleura and sternite of the ULBS, ventral view; (I) ultimate leg prefemur, dorsal view; (J) spiracle on segment 3; (K) spiracle on segment 5; (L) spiracle on segment 7; (M) spiracle on segment 8; (N): ultimate leg tarsus 2 and claw. (O) segment 21, coxopleura and ultimate leg, ventral lateral view. (P) paratype CMMI 20201209104, coxopleuron, lateral view. (A)–(P). Scale bar = 1 mm.

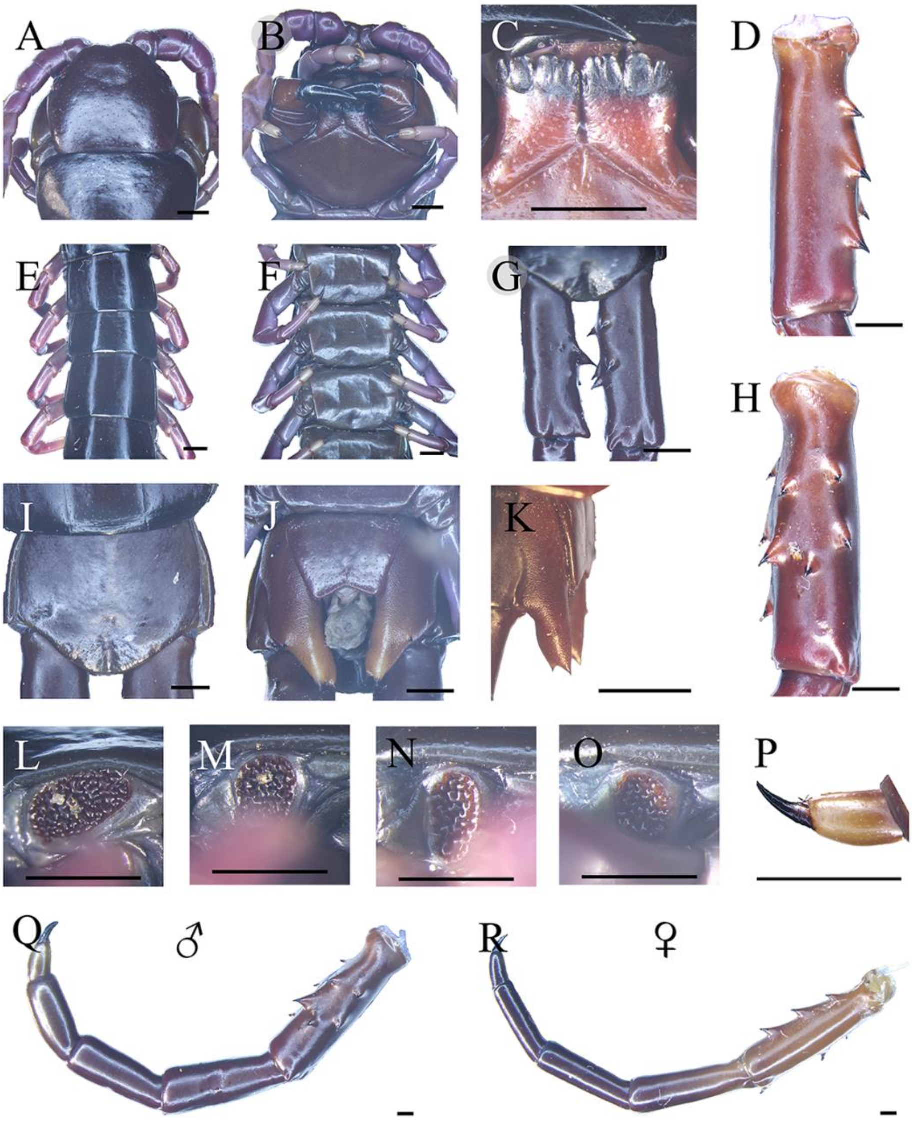

Figure 4. *Ethmostigmus austroyunnanensis* **sp. nov.** (A)–(Q) holotype CMMI 20200608081. (A) Cephalic plate, tergite T1, and proximal part of antennae, dorsal view; (B) cephalic plate and proximal part of antennae, ventral view, (C) tooth-plates, ventral view; (D) ultimate leg prefemur, ventral lateral view; (E) tergites 9–12; (F) sternites 7–10; (G) ultimate leg prefemur, dorsal view; (H) ultimate leg prefemur, ventral medial view; (I) tergite of the ultimate leg-bearing segment (ULBS), dorsal view; (J) coxopleura and sternite of the ULBS, ventral view; (K) coxopleuron, lateral view, scale = 1 mm; (L) spiracle on segment 3; (M) spiracle on segment 5; (N) spiracle on segment 7; (O) spiracle on segment 8; (P): ultimate leg tarsus 2 and claw. (Q) ultimate leg, ventral lateral view; (R) paratype CMMI 20201209104, ultimate leg, ventral lateral view. (A)–(R). Scale bar = 1 mm.

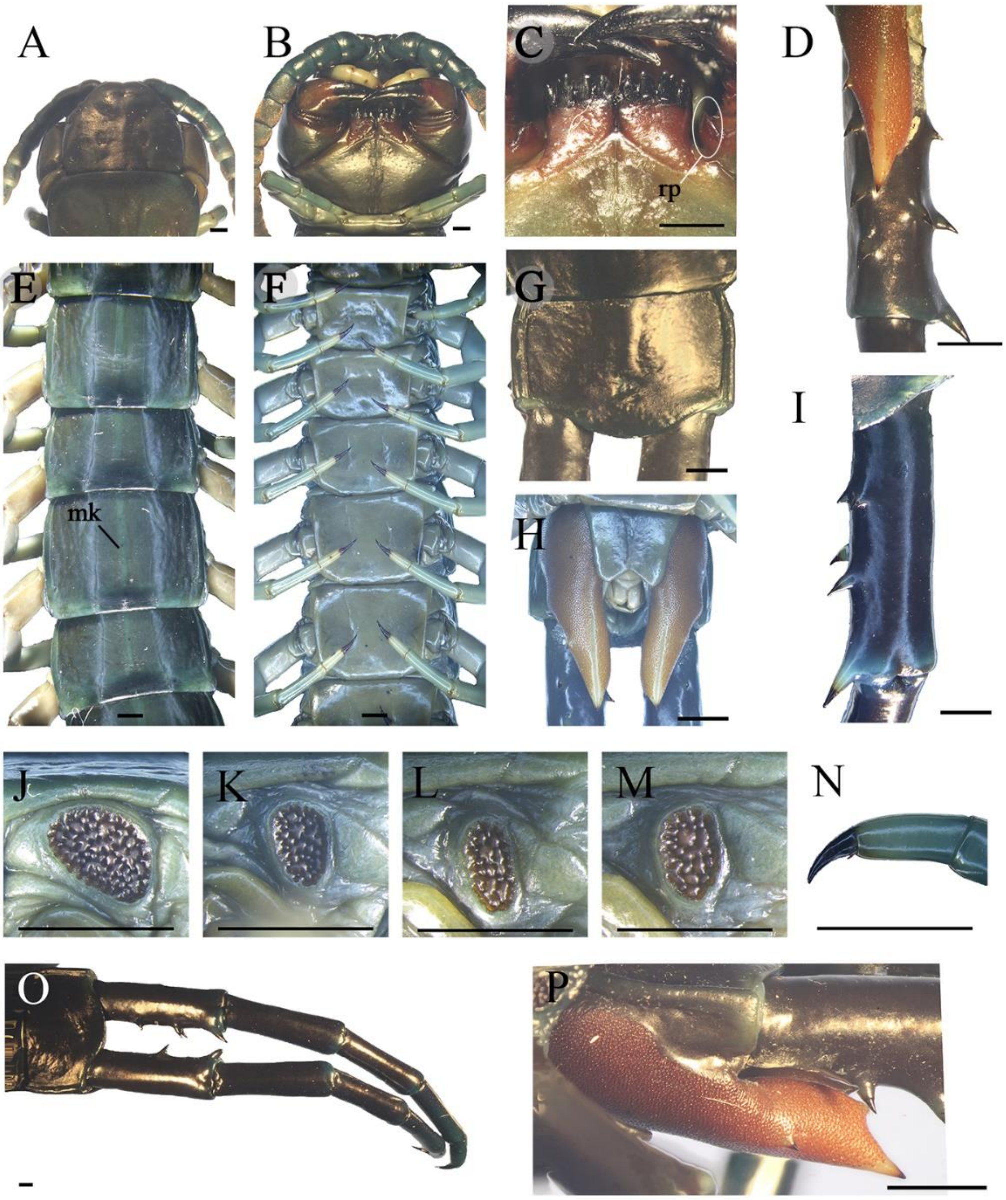

Figure 5. *Ethmostigmus biocolor* **sp. nov.** holotype CMMI 20200608081. (A) Cephalic plate, tergite T1, and proximal part of antennae, dorsal view; (B) cephalic plate and proximal part of antennae, ventral view, (C) tooth-plates, ventral view; (D) ultimate leg prefemur, dorsal view; (E) tergites 9–12, dorsal view; (F) sternites 6–10, ventral view; (G) tergite of the ultimate leg-bearing segment, dorsal view; (H) coxopleuron and ultimate sternite, ventral view; (I) ultimate leg prefemur, ventral view; (J) spiracle on segment 3; (K) spiracle on segment 5; (L) spiracle on segment 7; (M) spiracle on segment 8; (N): ultimate leg tarsus 2 and claw. (O) ultimate leg, dorsal view; (P) coxopleuron, lateral view. rp, rudimentary forcipular trochanteroprefemoral process. mk, median keel. Scale bar = 1 mm.

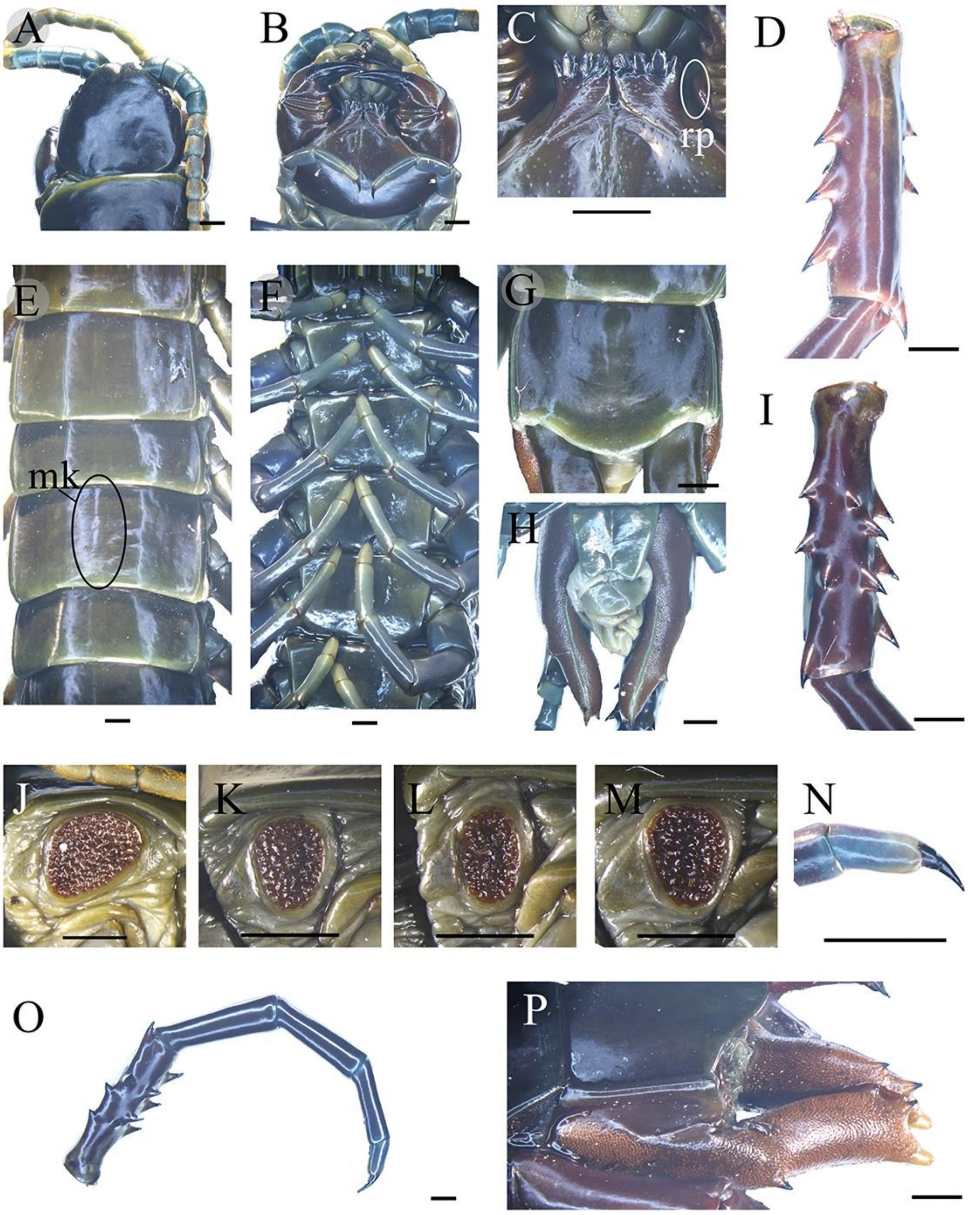

Figure 6. *Ethmostigmus motuonesis* **sp. nov.** (A) Cephalic plate, tergite T1, and proximal part of antennae, dorsal view; (B) cephalic plate, the first legs, and proximal part of antennae, ventral view, (C) tooth-plates, lateral view; (D) ultimate leg prefemur, ventral view; (E) tergites 9–12, dorsal view; (F) sternites 6–9, ventral view; (G) tergite of the ultimate leg-bearing segment, dorsal view; (H) coxopleuron and ultimate sternite, ventral view; (I) ultimate leg prefemur, ventral view; (J) spiracle on segment 3; (K) spiracle on segment 5; (L) spiracle on segment 7; (M) spiracle on segment 8; (N): ultimate leg tarsus 2 and claw. (O) ultimate leg, dorsal view; (P) coxopleuron, lateral view. (A)–(C), (E)–(M), paratype CMMI 20210316107. (D), (I), (N), (O), (P), holotype CMMI 20211008105. rp, rudimentary forcipular trochanteroprefemoral process. mk, median keel. Scale bar = 1 mm.

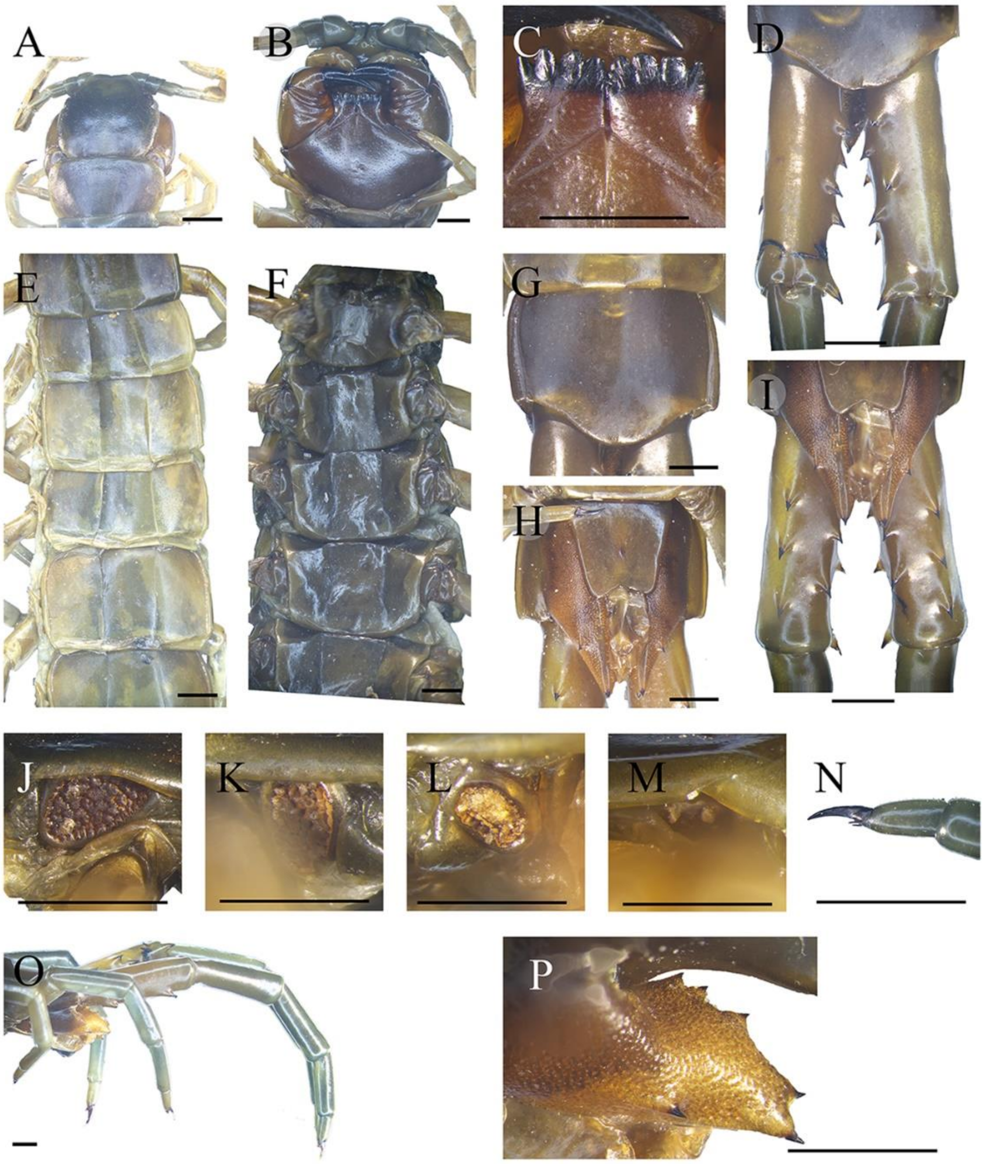

Figure 7. *Ethmostigmus pygomenasoides* Lewis, 1992 **stat. nov.** specimen CMMI 20200905127. (A) Cephalic plate, tergite T1, and proximal part of antennae, dorsal view; (B) cephalic plate, the first legs, and proximal part of antennae, ventral view, (C) tooth-plates, lateral view; (D) ultimate leg prefemur, dorsal view; (E) tergites 9–12, dorsal view; (F) sternites 5–8, ventral view; (G) tergite of the ultimate leg-bearing segment, dorsal view; (H) coxopleuron and ultimate sternite, ventral view; (I) ultimate leg prefemur, ventral view; (J) spiracle on segment 3; (K) spiracle on segment 5; (L) spiracle on segment 7; (M) spiracle on segment 8; (N): ultimate leg tarsus 2 and claw. (O) coxopleuron, leg 20 and ultimate leg, lateral view; (P) coxopleuron, lateral view. Scale bar = 1 mm.

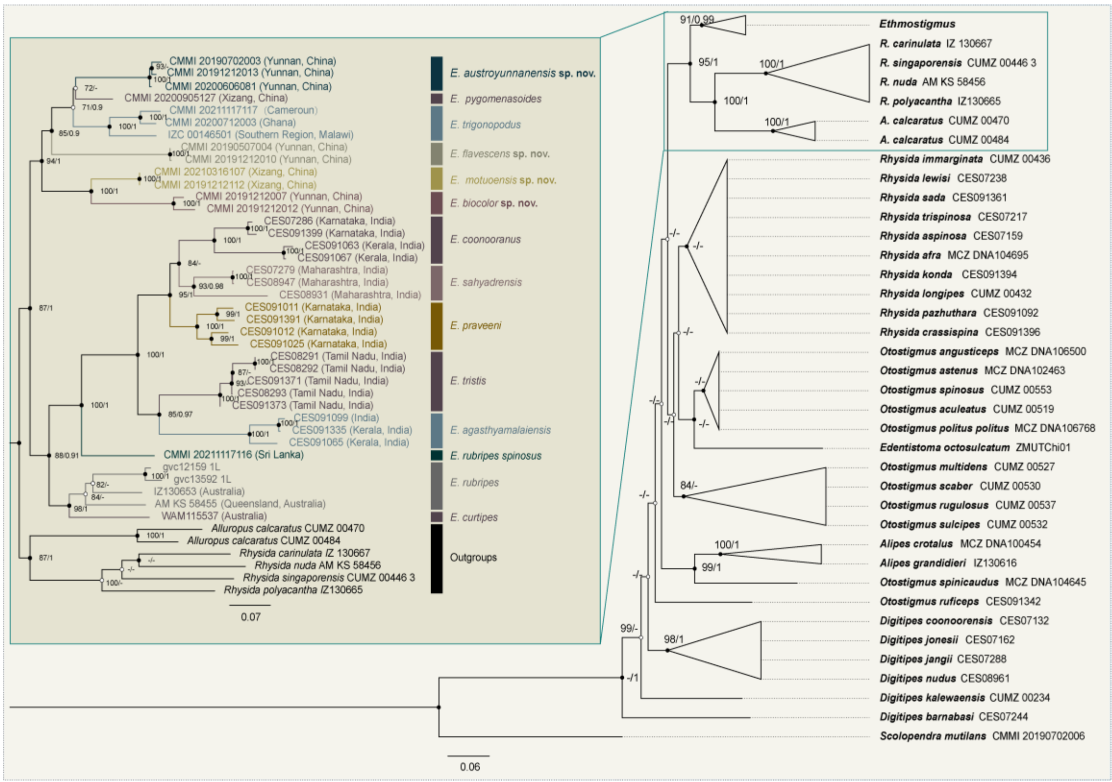

Figure 8. Maximum likelihood phylogenetic tree based on combined data for *Ethmostigmus* with likelihood bootstrap (BS > 70%) and Bayesian posterior probability (PP > 0.9) values indicated for each node. Specimen codes in parentheses denote the localities listed in Table 1.

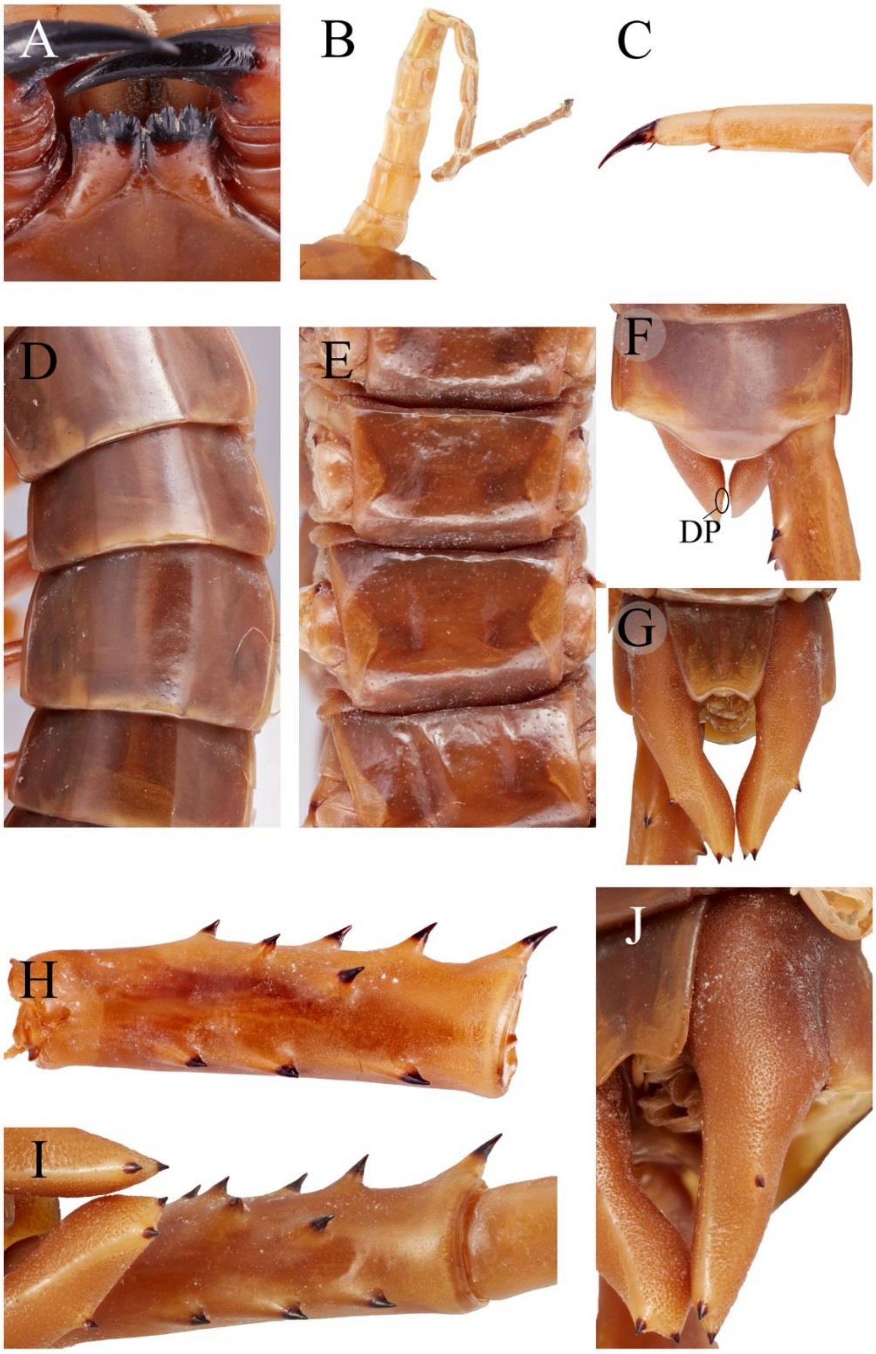

Figure 9. Syntypes of *E. pygomegas* (Kohlrausch, 1879), specimen ZMH-A0000640, 1 jar and 1 vial. Jar label: *Heterostoma rapax* Gerv. Original zu *H. pygomela* Kohlr. Himalaya (pencil). Vial label: *Heterostoma pygomega* n. sp. (pencil on red paper) [Godeffroy number: 31796]. (A) tooth-plates, ventral view; (B) right antennae, dorsal view; (C) proximal leg; (D) tergites, dorsal view; (E) sternite, ventral view; (F) tergite of the ultimate leg-bearing segment, dorsal view; (G) coxopleuron and ultimate sternite, ventral view; (H, I) ultimate leg prefemur, ventral view; (J) coxopleuron, lateral view. DP, dorsal spine. Credit: Nadine Dupérré.

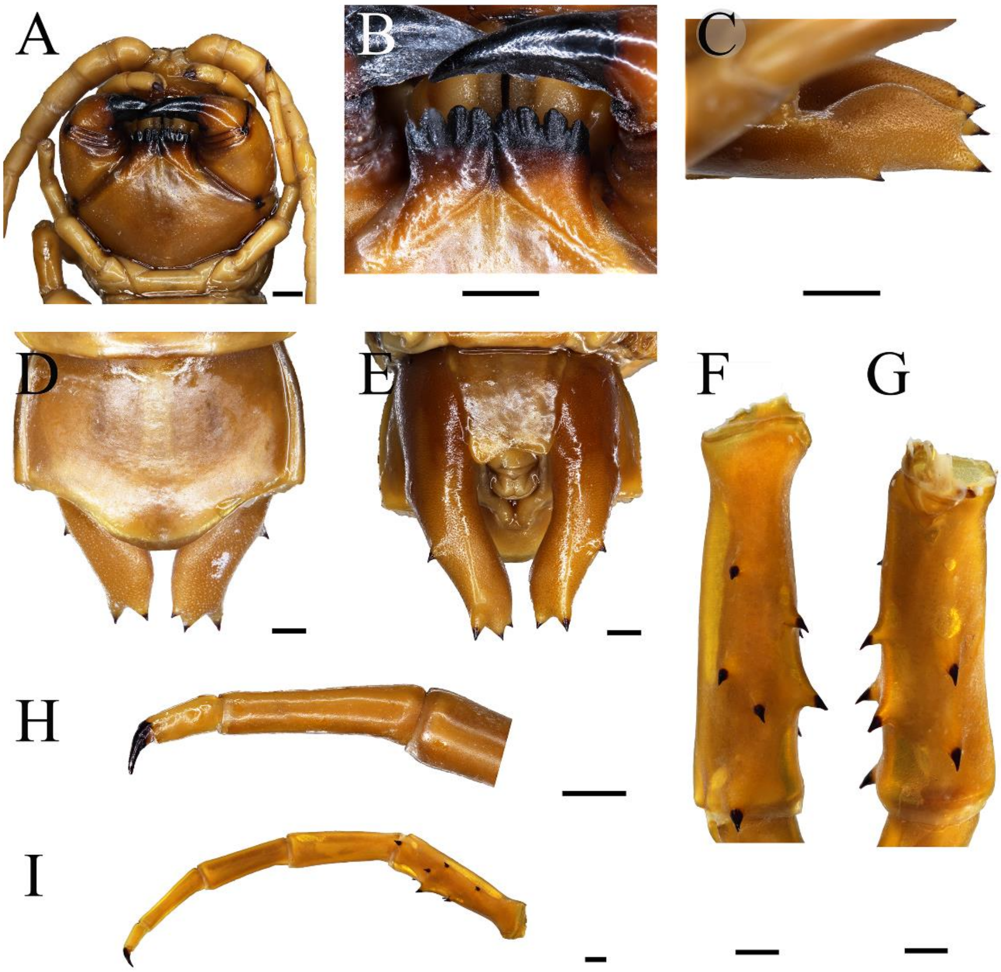

Figure 10. Syntype of *E. pygomegas* (Kohlrausch, 1879), specimen NHMW MY1561, 1 Ex., Originally labelled as *Heterostoma rapax* (pencil), Himalaya, [1882.I.14], [Godeffroy number: 14946]. (A) Cephalic plate, the first legs, and proximal part of antennae, ventral view; (B) tooth-plates, ventral view; (C) coxopleuron, lateral view; (D) tergite of the ultimate leg-bearing segment, dorsal view; (E) coxopleuron and ultimate sternite, ventral view; (F) ultimate leg prefemur, ventral lateral view; (G) ultimate leg prefemur, ventral medial view; (H) ultimate leg tarsus and claw; (I) ultimate leg, ventral medial view. Scale bar = 1 mm. Credit: Oliver Macek.

Table 1 Samples used for phylogenetic analyses

No.	Species	Voucher number	Taxon locality	GenBank accession number COI	16S	28S	Reference
1	*Ethmostigmus flavescens*	CMMI 20191212010	China: Yunnan: Mengla	ON231521	ON232473	ON232460	This study
2	*Ethmostigmus flavescens*	CMMI 20190507004	China: Yunnan: Mengla	ON231522	ON232474	ON232461	This study
3	*Ethmostigmus austroyunnanensis*	CMMI 20201214112	China: Yunnan: Yingjiang	ON231523	ON232475	ON232462	This study
4	*Ethmostigmus austroyunnanensis*	CMMI 20190702003	China: Yunnan: Yingjiang	ON231524	ON232476	ON232463	This study
5	*Ethmostigmus austroyunnanensis*	CMMI 20200606081	China: Yunnan: Mangshi	ON231525	ON232477	ON232464	This study
6	*Ethmostigmus motuoensis*	CMMI 20210316107	China: Xizang: Motuo	ON231526	ON232478	ON232465	This study
7	*Ethmostigmus motuoensis*	CMMI 20190712112	China: Xizang: Motuo	ON231527	ON232479	ON232466	This study
8	*Ethmostigmus bicolor*	CMMI 20191212007	China: Yunnan: Yingjiang	ON231519	ON232471	ON232458	This study
9	*Ethmostigmus bicolor*	CMMI 20191212012	China: Yunnan: Yingjiang	ON231520	ON232472	ON232459	This study
10	*Ethmostigmus pygomenasoides*	CMMI 20200905127	China: Xizang: Jilong	-	ON232480	-	This study
11	*Ethmostigmus rubripes spinosus*	CMMI 20211117116	Sri Lanka	ON231528	ON232481	ON232467	This study
12	*Ethmostigmus trigonopodus*	CMMI 20200712003	Ghana	ON209601	ON209448	ON212678	This study
13	*Ethmostigmus trigonopodus*	CMMI 20211117117	Cameroun	ON209602	ON209449	ON212679	This study
14	*Ethmostigmus agasthyamalaiensis*	CES091065	India: Kerala: Parambikulam Tiger Reserve	MH908726	MH908695	MH908710	1
15	*Ethmostigmus agasthyamalaiensis*	CES091099	India: Shendurney Wildlife Sanctuary: Pandimatte	MH908728	MH908696	MH908711	1
16	*Ethmostigmus agasthyamalaiensis*	CES091335	India: Kerala: Kottavasal Reserve Forest	MH908729	MH908697	MH908712	1
17	*Ethmostigmus coonooranus*	CES091067	India: Kerala: Parambikulam Tiger Reserve	MH908727	MH908693	-	1
18	*Ethmostigmus coonooranus*	CES091063	India: Kerala: Parambikulam Tiger Reserve	MH908725	MH908692	-	1
19	*Ethmostigmus coonooranus*	CES091399	India: Karnataka: Bramhagiri Wildlife Sanctuary	-	MH908694	MH908709	1
20	*Ethmostigmus coonooranus*	CES07286	India: Karnataka: Coorg	JN004031	JN003920	-	1
21	*Ethmostigmus praveeni*	CES091011	India: Karnataka: Kudremukh National Park	MH908722	MH908686	MH908703	1
22	*Ethmostigmus praveevni*	CES091012	India: Karnataka: Kudremukh National Park	MH908723	MH908687	MH908704	1

23	*Ethmostigmus praveeni*	CES091025	India: Karnataka: Shimoga	MH908724	MH908688	MH908705	1
24	*Ethmostigmus praveeni*	CES091391	India: Karnataka: Sakaleshapur Reserve Forest	MH908731	MH908689	MH908706	1
25	*Ethmostigmus sahyadrensis*	CES08931	India: Maharashtra: Mahabaleshwar Reserve Forest	MH908720	MH908690	MH908707	1
26	*Ethmostigmus sahyadrensis*	CES08947	India: Maharashtra: Sindhudurg	MH908721	MH908691	MH908708	1
27	*Ethmostigmus sahyadrensis*	CES07279	India: Maharashtra: Sindhudurg	JN004030	JN003919	JN003975	1
28	*Ethmostigmus trigonopodus*	IZC 00146501	Malawi: Southern Region: Zonba	HQ402547	HQ402495	-	2
29	*Ethmostigmus tristis*	CES08291	India: Tamil Nadu: Namakkal	MH908717	MH908698	MH908713	1
30	*Ethmostigmus tristis*	CES08292	India: Tamil Nadu: Namakkal	MH908718	MH908699	MH908714	1
31	*Ethmostigmus tristis*	CES08293	India: Tamil Nadu: Namakkal	MH908719	MH908700	-	1
32	*Ethmostigmus tristis*	CES091373	India: Tamil Nadu: Namakkal	-	MH908702	MH908716	1
33	*Ethmostigmus tristis*	CES091371	India: Tamil Nadu: Namakkal	MH908730	MH908701	MH908715	1
34	*Ethmostigmus rubripes*	gvc13592-1L	-	HQ986501	-	-	Genbank
35	*Ethmostigmus rubripes*	gvc12159-1L	-	HQ986492	-	-	Genbank
36	*Ethmostigmus rubripes*	AM KS 58455	Australia: Queensland: Lizard Island	AF370836	AY288721	AF173281	2
37	*Ethmostigmus rubripes rubripes*	IZ130653	Australia	KF676542	KF676475	KF676373	3
38	*Ethmostigmus curtipes*	WAM115537	Australia	KF676515	KF676474	KF676372	3
39	*Alipes grandidieri*	IZ130616	Tanzania	KF676514	KF676473	KF676371	3
40	*Alipes crotalus*	MCZ DNA100454	Swaziland	AY288742	AY288720	HM453273	2
41	*Alluropus calcaratus*	CUMZ 00470	Laos: Ban NamHom: Xieang Khuang	MF167838	MF167771	MF167905	5
42	*Alluropus calcaratus*	CUMZ 00484	Thailand: Surat Thani: Donsak	MF167821	MF167754	MF167888	5
43	*Digitipes barnabasi*	CES07244	India: GoaKarnataka border: Dughsagar Water Falls	JX531837	JX531707	JX531784	6
44	*Digitipes coonoorensis*	CES07132	India: Kerala: New Amarambalam Wildlife Sanctuary	JN004035	JN003924	JN003981	7
45	*Digitipes jangii*	CES07288	India: Karnataka: Kodagu	JX531839	JX531709	JX531786	6
46	*Digitipes jonesii*	CES07162	India: Kerala: Thiruvananthapuram	JN004042	JN003931	JN003986	7
47	*Digitipes kalewaensis*	CUMZ 00234	Myanmar: Sagaing Division: Kale	KP204116	KP204112	–	5
48	*Digitipes nudus*	CES08961	India: Kerala: Idukki	MK273245	MK273357	MK273467	1

49	*Edentistoma octosulcatum*	ZMUTChi01	Sarawak, Malaysia	KM492931	KM492929	KM492928	8
50	*Otostigmus aculeatus*	CUMZ 00519	Laos: Huaphan: Mueang Yommarat	MF167797	MF167730	MF167864	5
51	*Otostigmus angusticeps*	MCZ DNA106500	Papua New Guinea: Finisterre Mountains	KF676509	–	KF676365	3
52	*Otostigmus astenus*	MCZ DNA102463	Fiji/Vanuatu	HM453312	HM453221	HQ402532	2
53	*Otostigmus multidens*	CUMZ 00527	Thailand: Chiang Mai: Mae Taeng	MF167795	MF167728	MF167862	5
54	*Otostigmus politus politus*	MCZ DNA106768	China: Henan: Dengfeng	KF676512	KF676470	KF676368	3
55	*Otostigmus ruficeps*	CES091342	India: Kerala: Kollam	JX531901	JX531771	JX531822	6
56	*Otostigmus rugulosus*	CUMZ 00537	Thailand: Nan: Phu Phiang	MF167787	MF167720	MF167854	5
57	*Otostigmus scaber*	CUMZ 00530	Laos: Luang Phrabang: Wat Ban Hu	MF167802	MF167735	MF167869	5
58	*Otostigmus spinicaudus*	MCZ DNA104645	Tunisia: Kasserine	–	KF676472	KF676370	3
59	*Otostigmus spinosus*	CUMZ 00553	Thailand: Nakhon Si Thammarat: Khanom	MF167785	MF167718	MF167852	5
60	*Otostigmus sulcipes*	CUMZ 00532	Thailand: Chiang Mai: Huai Hong Khrai	MF167803	MF167736	MF167870	5
61	*Rhysida afra*	MCZ DNA104695	South Africa: Eastern Cape	HQ402552	HQ402500	HQ402536	2
62	*Rhysida aspinosa*	CES07159	India: Kerala: Thiruvananthapuram	MK273209	MK273316	MK273437	6
63	*Rhysida carinulata*	IZ-130667	Papua New Guinea: Western Province	KF676516	–	KF676374	3
64	*Rhysida crassispina*	CES091396	India: Maharashtra: Matheran	MK273288	MK273412	MK273508	6
65	*Rhysida immarginata*	CUMZ 00436	Thailand: Ranong: Kra Buri	MF167826	MF167759	MF167893	5
66	*Rhysida konda*	CES091394	India: Odisha: Koraput	MK273286	MK273410	MK273506	6
67	*Rhysida lewisi*	CES07238	India: Karnataka: Uttara Kannada	JN004024	JN003913	JN003969	6
68	*Rhysida longipes*	CUMZ 00432	Myanmar: Bahin village: PK2	MF167833	MF167766	MF167900	5
69	*Rhysida nuda*	AM KS 58456, IZ130678	Australia: New South Wales	DQ201432	AY288722	AF173282	2
70	*Rhysida pazhuthara*	CES091092	India: Kerala: Kollam district	MK273268	MK273386	MK273488	6
71	*Rhysida polyacantha*	IZ130665	Australia: Northern Territory	KF676518	KF676476	KF676376	3
72	*Rhysida sada*	CES091361	India: Maharashtra: Raigad	MK273279	MK273402	MK273499	6
73	*Rhysida singaporensis*	CUMZ 00446.3	Singapore: Bukit Timah	MF167844	MF167777	MF167911	5
74	*Rhysida trispinosa*	CES07217	India: Karnatka: Uttara Kannada	MK273214	MK273322	MK273441	6

75	*Scolopendra mutilans*	CMMI 20190702006	China: Taiwan: Kenting	MT093846	MT084409	MT084375	4

1 = Joshi & Edgecombe 2019a; 2 = Vahtera et al. 2012; 3 = Vahtera et al. 2013; 4 = Jiang et al. 2020; 5 = Siriwut et al. 2018; 6 = Joshi et al. 2020; 7= Joshi & Karanth 2011; 8 = Vahtera & Edgecombe 2014;

Table 2. Comparison of the morphologies of *Ethmostigmus* centipedes from China. Prefemoral spine formula on ultimate legs: VL: ventrolateral spine, VM: ventromedial spine, M: median spine, DM: dorsomedial spine, SP: spine on prefemoral process/prefemoral corner process. UL: ultimate leg. Reference: 1 = this study, 2 = lewis 1992, 3 = Thofern et al. 2021, 4 = Kohlrausch 1879.

Characters	*E. flavescens*	*E. austroyunnanensis*	*E. biocolor*	*E. motuoensis*	*E. pygomenasoides*		*E. pygomegas*
Ref	1	1	1	1	1	2	1, 3, 4
Locality	Yunnan	Yunnan	Yunnan	Xizang	Xizang	Nepal	Himalaya, Bhutan; India; Myanmar
Body length (mm)	75–90	81–101	76–108	87–110	73	28–100	reach 120
Number of antennal articles	20	10	20	20	20	?	20
Number of glabrous articles (dorsal/ventral)	4/3	4/3	4/3	4/3	4/3	4/3	4/3
Main teeth on tooth plate	4	4	4	4	4	4	4
Rudimentary forcipular trochanteroprefemoral process	absent	absent	present	present	absent	absent	absent
Length: wide of tooth plate	1.68–2.02:1	1.66–1.83:1	1.32–1.38:1	1.37–1.46:1	1.27(R), 1.48(L)	1.40–1.57	1.52–1.68
First tergite with complete paramedian sutures	4–5	3–4	2–3(4)	4–5(8)	3	3–4	?
First tergite margin complete	5–6	4–6	4–6	4–5	3	5–6	?

Tergites with median keel	absent	absent	6(8)–21	7(8)–21	absent	absent	incomplete or absent
Paramedian sutures on sternites complete	2–3	3–5	2–3	incomplete	2	ranging from short anterior to virtually complete	incomplete
Spines on coxopleural process: AP, SAP, DP, LP	AP2, DP 1(0), LP1	AP2, LP1	AP1, SAP1, LP1	AP1, SAP1, DP 1(0), LP1(2)	AP2, DP 3, LP1	AP2, DP 1–4, LP1(0)	AP1, SAP1, DP 0–1, LP1
Length of coxopleural process: S21	2.28–2.81	1.6–1.86	2.38–2.78	2.70–3.12	2.03	1.77–2.27	2.47–2.61
VL	2	3	3(4)	3(2)	3	2–3	2–3
VM	2(1)	2	2(1)	2(3)	2	1–2	2
M	1(2)	1	2(2)	2	2	1?	1–2
DM	2	2	2	2(3)	2	1–2	2
Total spines	7	8	9(8)	9(10)	9	8?	7–9
Width: Length of T21	1.50–1.64	1.41–1.65	1.79–1.91	1.36–1.52	1.32	?	1.56–1.64
Length of prefemur: femur	1.26–1.44	1.18–1.23	1.05–1.35	1.21–1.39	1.29	?	1.33
Length of femur: tibia	1.22–1.30	1.16–1.28	1.22–1.28	1.04–1.13	1.17	?	1.22
Length of tibia: tarsus 1	1.3–1.44	1.24–1.28	1.15–1.30	1.12–1.34	1.32	?	1.17
Length of tarsus 1: tarsus 2	2.25–2.50	2.05–2.38	1.92–2.21	2.13–2.32	1.95	?	2.63
Legs with two tarsal spurs	1 to (2)3–4	1 to 2–3	1(2)	1(0)	1	1	1
Legs with one tarsal spur	(3)4–5 to 19	3–4 to 20	2(3)–20	2(1)–19(20)	2–20	2–20	2–19

ARPHA Preprints Author-formatted, not peer-reviewed document posted on 13/05/2022 DOI: https://doi.org/10.3897/arphapreprints.e86382

Legs with femoral spur	1	1	1(0)	0(1)	0	?	1
Legs with tibial spur	1	1	1(0)	1(0)	1	?	1
Claw spines on UL	0(1)	2	2(1)	0(1)	2	2	0